SOME RECENT RESULTS WITH NONNEUTRAL PLASMAS

J.H. Malmberg[1]

Department of Physics, University of California, San Diego
La Jolla, California 92093-0319

ABSTRACT

Two examples of recent research using pure electron plasmas are discussed. Various phenomena of two-dimensional fluid dynamics were investigated including vortex dynamics, vortex merger, shear-induced instability, and the decay of turbulence. In a second series of experiments, the rate at which the temperatures parallel and perpendicular to a magnetic field relax to a common value has been measured over a very wide range in temperatures and magnetic fields.

KEYWORDS

Nonneutral plasma; vortex dynamics; vortex merger; collisions; adiabatic invariants.

INTRODUCTION

In recent years many groups have been studying the properties of plasmas for which all the particles have the same sign of charge. These plasmas are unusually simple both experimentally and theoretically, but they nevertheless exhibit a wide range of collective phenomena. Experiments and theory concerned with equilibrium, stability, waves, 2D fluid mechanics, collisions, a wide range of transport phenomena, and crystallization at low temperature have been carried out in many laboratories. It is not possible to review this body of work in a single lecture, and it should not be inferred that the present lecture is intended as a scholarly review of the field. Instead I will restrict my remarks to summarizing research on pure electron plasmas at UCSD in two areas, namely, two-dimensional fluid mechanics and collisional relaxation of an anisotropic temperature.

The geometry and measurement techniques for pure electron plasmas have been previously described (Malmberg et al., 1988). The electron plasma is contained in a series of grounded conducting cylinders, as shown schematically in Fig. 1. A uniform axial magnetic field provides radial confinement, and negative voltages applied to end cylinders provide axial confinement. The electron plasma contains a negligible number of positive ions, since ions are not confined longitudinally. The magnetized column of electrons is a plasma by the criterion that the Debye length is small compared to the radius of the column. The apparatus is operated in an inject-manipulate-dump cycle. For injection, the leftmost cylinder is briefly grounded, allowing electrons to enter from the negatively biased tungsten filament source. The trapped electrons can then be manipulated by applying voltages to various sections of the cylindrical wall. Typically, we manipulate the plasma to create the desired "initial condition," then study the resulting evolution.

---

[1] In collaboration with B.R. Beck, C.F. Driscoll, J. Fajans, K.S. Fine, M.E. Glinsky, R.W. Gould, P.G. Hjorth, X-P. Huang, A.W. Hyatt, S. Ichimaru, T.B. Mitchell, T.M. O'Neil, M.N. Rosenbluth, R.A. Smith, and K. Tsuruta.
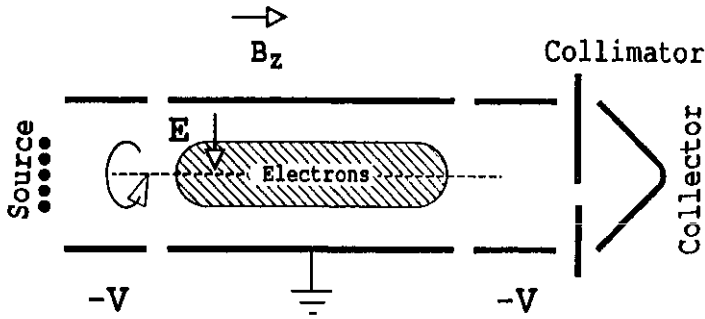
Fig. 1.   Simplified schematic of the confinement device.

At any time t during the evolution, the z-averaged electron density $n(r,\theta,t)$ can be measured by grounding the rightmost cylinder, thereby dumping the electrons. The temporal dependence is obtained by varying the evolution time t on successive cycles; and the spatial dependence is obtained by varying the position r of the radially scanning collimator hole, and the phase θ of the initial condition. Of course, this imaging process relies on a high shot-to-shot reproducibility in the plasma initial conditions; typically we have less than 1% shot-to-shot variation in the measured dumped charge at a particular (r,θ) and $t=0$.

The parallel temperature of the confined plasma is measured by collecting the electrons which are energetic enough to escape past the confinement potential applied to the rightmost cylinder as this potential is slowly made less negative. The perpendicular temperature of the plasma is measured by determining how much the parallel velocity distribution of the dumped electrons is changed as they pass through a cusp or mirror which converts some perpendicular energy to parallel energy or vice versa (Hsu and Hirschfield, 1976; deGrassie, 1977).

2D FLUID DYNAMICS

If the axial bouncing of the individual electrons averages over any z-variations at a rate fast compared to $r-\theta$ drifts, then the electron dynamics can be approximated by 2-dimensional guiding center theory. If viscosity is neglected, the 2D drift-Poisson equations for the electron column are isomorphic to the 2D Euler equations for an inviscid fluid of uniform density (Levy, 1965, 1968; Briggs et al., 1970; Driscoll and Fine, 1990). In the plasma case the electrostatic potential $\phi(r,\theta)$ arises from the charge density $n(r,\theta)$ through Poisson's equation, and the resulting $\mathbf{E}\times\mathbf{B}$ drift velocities give incompressible flow. This is isomorphic to inviscid incompressible fluid flow characterized by a stream function $\psi(r,\theta)$. The vorticity $\Omega(r,\theta)$ of the flow is proportional to $\nabla^2\phi$ (or $\nabla^2\psi$). In the electron system only, this vorticity is also proportional to the density $n(r,\theta)$, which we measure directly. The continuity equation for electrons and the momentum equation for the fluid then both give the same evolution equation, i.e. that the convective derivative of the vorticity is zero. The boundary conditions are also equivalent, namely $\phi=$constant and $\psi=$constant on the cylindrical walls. One advantage of the electron experiments for testing 2D fluid theory is that the electron system tends to remain 2D, due to the magnetic field. Another advantage is that the electron column has low internal viscosity and has no boundary layers at the cylindrical walls or ends.

Vortex Dynamics

The interaction of two extended vortices is one of the most fundamental processes in 2D fluid dynamics, and the electron plasma is well-suited to studying this process. Various manipulation techniques allow the formation of an initial condition consisting of two electron columns of chosen

profile and placement. The particular case of two equal columns which are placed symmetrically on either side of the cylindrical axis has been studied experimentally (Driscoll and Fine, 1990; Fine *et al.*, 1991). The behavior of the two vortices depends dramatically on their initial separation to diameter ratio. If the vortices are separated by more than 1.8 diameters, they orbit around each other relatively unperturbed for up to 10^4 orbits. If the vortices are initially separated by 1.6 diameters, their mutual interaction quickly results in filamentary tail formation, but the vortices still orbit around each other for about 100 orbits before merging. If they are separated by 1.5 diameters, we observe merger at the center in less than one orbit period. This case is shown in Fig. 2.
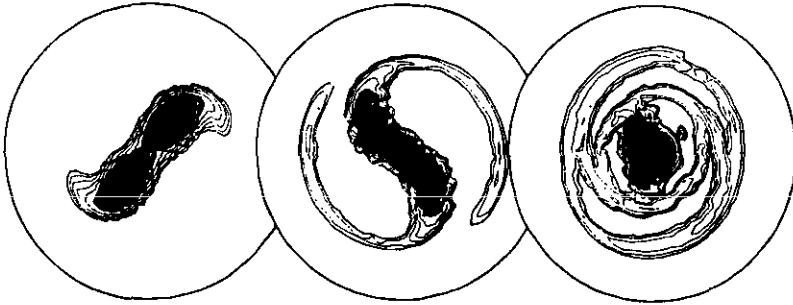

Fig. 2.   Measured contour plots of density (or vorticity) during vortex merger. The three pictures are separated by 30-μsec intervals, and the eight contours are on a logarithm scale spanning 1 to 0.01. The outer circles represent the conducting wall.

A plot of the time required to merge versus the initial vortex separation is shown in Fig. 3. The merger time abruptly increases from 10 μsec to about 1 sec as the initial separation varies from 1.5 to 1.8 diameters. The merger time scales as the ratio of the vortex separation to the vortex diameter. The wall radius does not enter the scaling, indicating that the mutual interaction of the vortices dominates over wall interactions. These results are in agreement with two-dimensional fluid theory and simulations which predict a critical separation of $2D/2R_v$ between 1.5 and 1.8 (Moore and Saffman, 1975; Rossow, 1977; Zabusky *et al.*, 1979; Saffman and Szeto, 1980), and with a more qualitative experiment in a water tank (Griffiths and Hopfinger, 1987). The upper limit of 1 second in Fig. 3 represents about 10^4 orbits. At this time the vortices which were initially too far apart to merge have expanded enough due to internal viscosity to reach the critical distance for merger.
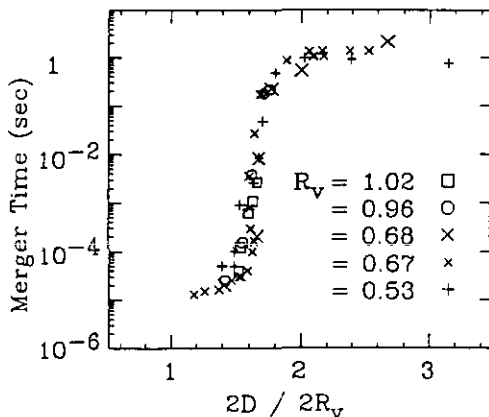

Fig. 3.   Experimentally measured merger time versus the initial ratio of vortex separation 2D to vortex diameter $2R_v$, for vortices of various diameters.

When the two vortices are sufficiently far apart so that they do not merge for thousands of rotations, the experiments show that their centers of mass move as expected for line vortices. In particular, a classical wall-induced orbit instability has been observed. This instability was considered for line vortices by Kelvin (1878) and J. J. Thompson (1883) and worked out in detail by T. H. Havelock (1931) but has not been previously observed. For line vortices surrounded by a cylindrical wall, the instability is predicted to occur only when the ratio of the orbit diameter to the wall diameter exceeds 0.46. The onset of the instability at the critical diameter is observed even though the experimental vortices are spatially extended rather than lines. The growth rate of the instability has also been measured and is in agreement with theory.

Shear-Flow Instabilities

If non-monotonic radial density profiles are created in long electron columns, the free energy in the shear of the drift rotation velocity drives strong Kelvin-Helmholtz instabilities of modes varying as $e^{il\theta}$ (Driscoll and Fine, 1990; Webster, 1955; Driscoll, 1990; Driscoll et al., 1989). On these hollow profiles two modes are observed for each l, with distinct frequencies and eigenfunctions, one stable and one unstable, rather than the complex pairs predicted by simple theory. When the eigenvalue equation is integrated numerically for realistic smooth density profiles, fair agreement with the measured frequencies and instability rates for $l = 2$ modes is obtained (Driscoll et al., 1989).

Exponential growth of the unstable $l = 1$ mode over a range of up to 2 decades is also observed before nonlinear saturation occurs. In contrast, prior theory (Levy, 1965, 1968) had concluded that there were no exponential instabilities for $l = 1$, and it was believed that the $l = 1$ modes were strictly stable. More recent theoretical work stimulated by the experiments has elucidated an $l = 1$ instability which grows algebraically with time (Smith and Rosenbluth, 1990), but not exponentially. The theoretical growth with time can be obtained by numerically integrating a linear Laplace transform solution or by asymptotic analysis, obtaining a perturbation proportional to $t^{1/2}$ as $t \rightarrow \infty$. This instability has also been studied using a 2D particle-in-cell simulation in which the particles (long rods parallel to the field) move according to $\mathbf{E} \times \mathbf{B}$ drift dynamics. The simulation results agree with analytic 2D theory. However, experiment and this theory disagree sharply on the amount and time dependence of the growth. Extension of the theory to include end effects due to finite length of the plasma predicts exponential growth of the mode at approximately the right rate (Smith, 1992). This theory is more ad hoc than from first principles, so the situation is not entirely satisfactory.

Shear-Induced Decay of Noise

The unstable modes grow exponentially until they saturate with the formation of nonlinear vortex structures. These vortices eventually merge at the center, leaving chaotic density variations on smaller spatial scales. Thus the instabilities result in large-scale cross-field transport which proceeds until the plasma is no longer unstable because its density profile has become approximately monotonically decreasing. The decay of the density variations in the approximately monotonically decreasing density profile has been studied. In these experiments the density is measured asynchronously with any internal processes, so variations in $n(r,\theta)$ appear as shot-to-shot noise. Long term noise and correlation measurements (Driscoll et al., 1989) elucidate how the system decays. An example of the RMS δn vs time is shown in Fig. 4a. The initial density variations at $r = 1$ cm are about 0.1% of the initially injected density there. By 100 μsec the instabilities have saturated, and RMS δn has risen to ~10%. The noise then decays exponentially to a plateau level in about 1 msec. Correlation measurements show that the θ-variations are decaying during this time, apparently due to shear in the rotation velocity pulling the initial density variations into long spirals. This is demonstrated by Fig. 4b which gives the correlation function between simultaneous density measurements 90° apart on a 1 cm radius as a function of time. After wild but real oscillations during the initial instability growth, the correlation goes from approximately zero at 200 μs to 100% at 1 msec, showing that the residual noise is θ-independent. The correlation between collectors 180° apart gives similar results.
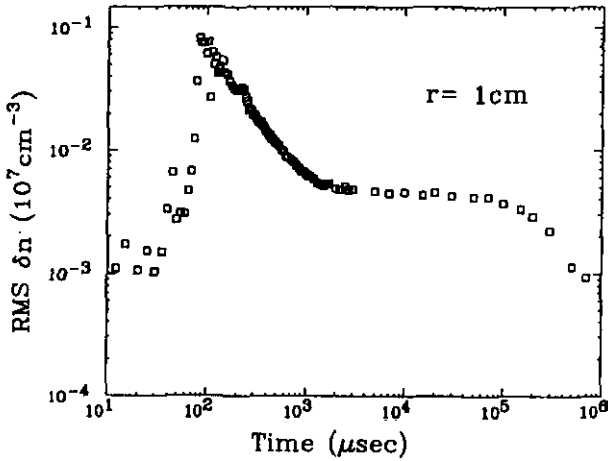
Fig. 4a. RMS shot to shot density fluctuations vs. time for the evolution of a hollow plasma.
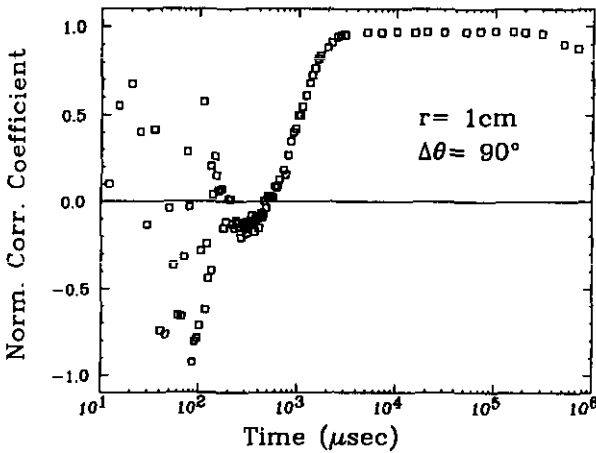

Fig. 4b. Normalized correlation coefficient for simultaneous density measurements on collectors at $r = 1$ cm but $90°$ apart.

This decay of the θ-dependent part of the noise is accurately exponential for about two decades. The decay time has been compared to a mean field theory based on the assumption that the density is simply a passive scaler which is being sheared by radial shear in the average rotation velocity. This theory predicts a noise decay about 5 times faster than is observed. This discrepancy suggests that patches of vorticity are rotating about their own axis and resist being torn apart by the overall shear. A detailed comparison with a hybrid theory suitable for this situation has not been made.

Radial density variations persist during the plateau from about 10^3 μsec to 10^5 μsec. Beginning at about 0.2 sec, the density fluctuations drop toward their initial 0.1% level, as slow transport smooths the radial profile.

COLLISIONAL RELAXATION

The collisional relaxation of a plasma with an anisotropic velocity distribution $(T_\parallel \neq T_\perp)$ is a funda-mental problem in plasma statistical mechanics. A recent series of experiments (Hyatt *et al.*, 1987;

Beck *et al.*, 1992) has measured the collisional relaxation of anisotropic thermal distributions, over a strikingly wide range of plasma parameters.

The influence of magnetic field strength on the collisional dynamics is parametrized by r_c/b, the ratio of the thermal cyclotron radius to the classical distance of closest approach. The plasma is weakly magnetized when $r_c/b \gg 1$, and strongly magnetized when $r_c/b \ll 1$. For the pure electron plasma, $r_c < \lambda_D$ in all cases. The equilibration rate ν is defined by $dT_\perp/dt = \nu(T_\parallel - T_\perp)$. For weak magnetization, early theory (Silin, 1961; Ichimaru and Rosenbluth, 1970; Montgomery *et al.*, 1974) predicts that the equilibration rate is the field-free rate, except that r_c replaces λ_D in the Coulomb logarithm, giving $\nu = (\sqrt{2\pi}/15) \, n\bar{v}b^2 \ln(r_c/b)$ where $\bar{v} = \sqrt{T/m}$. For strong magnetization, this expression obviously is not sensible, since $r_c/b < 1$. O'Neil and Hjorth (O'Neil, 1983; O'Neil and Hjorth, 1985) predicted that the collisional dynamics of a strongly magnetized plasma is constrained by a many-particle adiabatic invariant (the total cyclotron action, $\sum_j m v_{\perp j}^2/2\Omega_c$), and that this invariant makes the equilibration rate exponentially small. In particular, $\nu = n\bar{v}b^2 I(r_c/b)$, where $I(r_c/b) \sim \exp[-(2.34)(r_c/b)^{2/5}]$ (O'Neil and Hjorth, 1985). This analysis was corroborated by molecular dynamics simulations (Hjorth and O'Neil, 1987).

The precision and range of the measurements have motivated another iteration of the theory by Glinsky *et al.* (1992) providing a unified treatment that spans the whole range in r_c/b and matches onto asymptotic formulas in the two limits $r_c/b \gg 1$, and $r_c/b \ll 1$. A Boltzmann-like collision operator is used to obtain an integral expression for the rate. This reduces the problem of calculating the rate to the problem of calculating $\Delta E_\perp$, the change in the perpendicular kinetic energy that occurs during an isolated binary collision. In general, an analytic expression for $\Delta E_\perp$ cannot be obtained. Numerical solutions for $\Delta E_\perp$ are calculated for many initial conditions chosen at random, and the integral expression is evaluated by Monte Carlo techniques. The result of this theory is given as the solid line in Fig. 5, where the equilibration rate normalized to $n\bar{v}b^2$ is plotted against r_c/b.
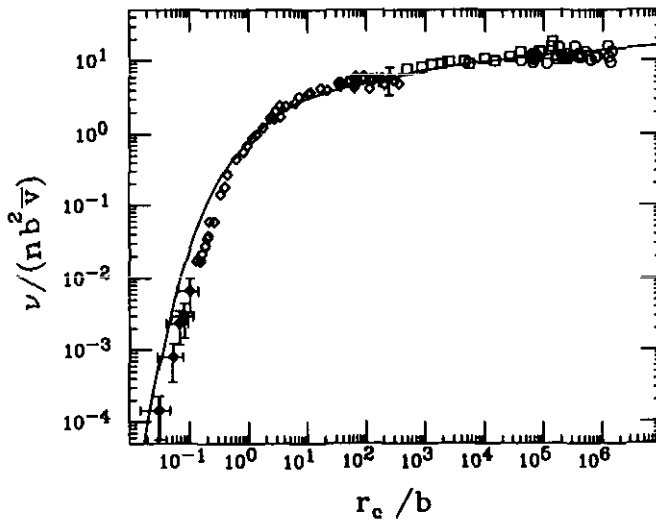

Fig. 5.   Normalized equilibration rate vs. r_c/b.

In two sets of experiments with pure electron plasmas, the equilibration rate has been measured over a range of 8 orders of magnitude in effective field strength r_c/b, as shown in Fig. 5. For the first experiment (Hyatt *et al.*, 1987), $T \sim 1\,\text{eV}$ and $B \sim 500\,\text{G}$, which is well in the regime of weak magnetization. To obtain this data, the electron plasma column is first allowed to evolve to an isothermal Maxwellian. A temperature anisotropy is then induced by applying potentials to cylinders to change the column length slowly compared to the axial bounce time yet rapidly compared to the collision time. This produces an essentially 1-D compression (or expansion) which changes $T_\parallel$ but not $T_\perp$. A

typical measured time evolution of $T_\parallel$ and $T_\perp$ during the subsequent relaxation is shown in Fig. 6. The relaxation rates are obtained as a function of plasma density and temperature by fitting data like that in Fig. 6. The results of this experiment are plotted as circles in the large r_c/b regime in Fig. 5.
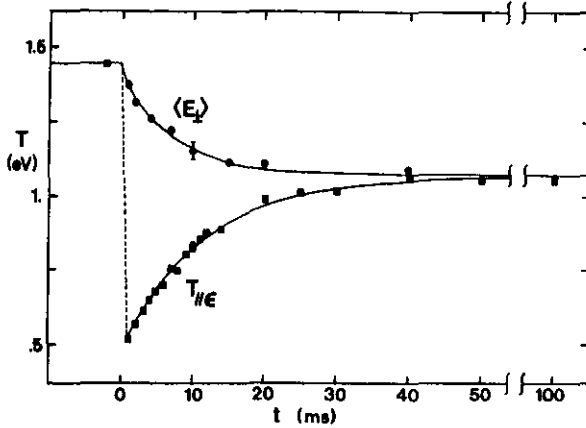

Fig. 6.   Relaxation to equilibrium of an anisotropic temperature
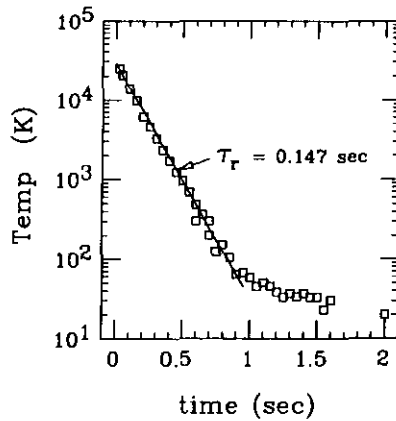   distribution.

Fig. 7.   Measured temperature versus time for $B = 61.3\,\text{kG}$.

Low temperature, high magnetic field results were obtained on a cryogenic apparatus (Beck et al., 1992), with $T \geq 0.002\,\text{eV}$, $B \leq 60\,\text{kG}$. In this experiment, the plasma can be strongly magnetized. For technical reasons, a somewhat different measurement technique was used for this experiment. In the high field regime, the temperature of the plasma falls toward the 4K cylinder temperature due to cyclotron radiation as shown in Fig. 7. When the desired temperature is reached, the plasma is heated by oscillating the containment voltage on the ends, and the equilibration rate is deduced by determining the frequency which produces the most heating at a given temperature. As the plasma temperature is reduced, the measured ν initially increases, peaks near $r_c = b$, and then sharply decreases. This decrease in ν for $r_c < b$ is consistent with the existence of the many electron adiabatic invariant. The experimental relaxation rates normalized to the basic collision frequency $n\,b^2\bar{v}$ are shown in Fig. 5. The measured rates agree with traditional theory over the parameter range $10^6 > r_c/b > 10$. As r_c/b goes from 10 down to 10^{-1}, the measured rates drop by over 4 decades, in close agreement with the new theory.

The comparison between theory and experiment in Fig. 5 illustrates the wide parameter range available with pure electron plasmas, and the advantages that the simplicity of these systems offers for a class of fundamental plasma experiments.

REFERENCES

Beck, B.R., J. Fajans and J.H. Malmberg (1992). Measurement of collisional anisotropic temperature relaxation in a strongly magnetized pure electron plasma. *Phys. Rev. Lett.* **68**, 317-320.

Briggs, R.J., J.D. Daugherty and R.H. Levy (1970). Role of Landau damping in crossed-field electron beams and inviscid shear flow. *Phys. Fluids* **13**, 421-432.

deGrassie, J.S. (1977). *Equilibrium, Waves and Transport in the Pure Electron Plasma.* Ph.D. dissertation (unpublished), pp. 81-86. Univ. of California, San Diego.

Driscoll, C.F., J.H. Malmberg, K.S. Fine, R.A. Smith, X.-P. Huang and R.W. Gould (1989). Growth and decay of turbulent vortex structures in pure electron plasmas. In: *Plasma Physics and Controlled Nuclear Fusion Research 1988*, Vol. 3, pp. 507-514. International Atomic Energy Agency, Vienna.

Driscoll, C.F. (1990). Observation of an unstable $l = 1$ diocotron mode on a hollow electron column. *Phys. Rev. Lett.* **64**, 645-648.

Driscoll, C.F. and K.S. Fine (1990). Experiments on vortex dynamics in pure electron plasmas. *Phys. Fluids B* **2**, 1359-1366.

Fine, K.S., C.F. Driscoll, J.H. Malmberg and T.B. Mitchell (1991). Measurements of symmetric vortex merger. *Phys. Rev. Lett.* **67**, 588-591.

Glinsky, M.E., T.M. O'Neil, M.N. Rosenbluth, K. Tsuruta and S. Ichimaru (1992). Collisional equipartition rate for a magnetized pure electron plasma. *Phys. Fluids B* **4**, 1156-1166.

Griffiths, R.W. and E.J. Hopfinger (1987). Coalescing of geostropic vortices. *J. Fluid Mech.* **178**, 73-97.

Havelock, T.H. (1931). *Phil. Mag.* (7) **11**, 617.

Hjorth, P.G. and T.M. O'Neil (1987). Numerical study of a many-particle adiabatic invariant. *Phys. Fluids* **30**, 2613-2615.

Hsu, T. and J.H. Hirschfield (1976). Electrostatic energy analyzer using a nonuniform axial magnetic field. *Rev. Sci. Instrum.* **47**, 236-238.

Hyatt, A.W., C.F. Driscoll and J.H. Malmberg (1987). Measurement of the anisotropic temperature relaxation rate in a pure electron plasma. *Phys. Rev. Lett.* **59**, 2975-2978.

Ichimaru, S. and M.N. Rosenbluth (1970). Relaxation processes in plasmas with magnetic field. Temperature relaxations. *Phys. Fluids* **13**, 2778-2789.

Kelvin (1878). *Math-Phys. Papers* iv, 135.

Levy, R.H. (1965). Diocotron instability in a cylindrical geometry. *Phys. Fluids* **8**, 1288-1295.

Levy, R.H. (1968). Two new results in cylindrical diocotron theory. *Phys. Fluids* **11**, 920-921.

Malmberg, J.H., C.F. Driscoll, B. Beck, D.L. Eggleston, J. Fajans, K.S. Fine, X.-P. Huang and A.W. Hyatt (1988). Experiments with pure electron plasmas. In: *Non-neutral Plasma Physics* (C.W. Roberson and C. F. Driscoll, eds.), AIP Conf. Proc. 175, pp. 28-71. American Institute of Physics, New York.

Montgomery, D., G. Joyce and L. Turner (1974). Magnetic field dependence of plasma relaxation times. *Phys. Fluids* **17**, 2201-2204.

Moore, D.W. and P.G. Saffman (1975). The density of organized vortices in a turbulent mixing layer. *J. Fluid Mech.* **69**, 465-473.

O'Neil, T.M. (1983). Collision operator for a strongly magnetized pure electron plasma. *Phys. Fluids* **26**, 2128-2135.

O'Neil, T.M. and P.G. Hjorth (1985). Collisional dynamics of a strongly magnetized pure electron plasma. *Phys. Fluids* **28**, 3241-3252.

Rossow, V.J. (1977). Convective merging of vortex cores in lift-generated wakes. *J. Aircr.* **14**, 283-290.

Saffman, P.G. and R. Szeto (1980). Equilibrium shapes of a pair of equal uniform vortices. *Phys. Fluids* **23**, 2339-2342.

Silin, V.P. (1961). The high frequency dielectric permeability of a plasma (English translation). *Zh. Eksp. Teor. Fiz.* **41**, 861-870. [High-frequency dielectric constant of a plasma. *Sov. Phys. JETP* **14**, 617-622.]

Smith, R.A. and M.N. Rosenbluth (1990). Algebraic instability of hollow electron columns and cylindrical vortices. *Phys. Rev. Lett.* **64**, 649-652.

Smith, R.A. (1992). Effects of electrostatic confinement fields and finite gyroradius on an instability of hollow electron columns. *Phys. Fluids* **4**, 287-289.

Thompson, J.J. (1883). *Treatise on Vortex Rings*, p. 94.

Webster, H.F. (1955). Breakup of hollow electron beams. *J. Appl. Phys.* **26**, 1386-1387.

Zabusky, N.J., M.H. Hughes and K.V. Roberts (1979). Contour dynamics for the Euler equations in two dimensions. *J. Comp. Phys.* **30**, 96-106.